Available online at www.sciencedirect.com
ScienceDirect
Journal of Power Sources 176 (2008) 340–346
JOURNAL OF POWER SOURCES
www.elsevier.com/locate/jpowsour

# Comb-like copolymer-based gel polymer electrolytes for lithium ion conductors

Yu-Hao Liang [a], Cheng-Chien Wang [b], Chuh-Yung Chen [a,*]

[a] *Department of Chemical Engineering, National Cheng-Kung University, Tainan 70148, Taiwan*
[b] *Department of Chemical and Material Engineering, Southern Taiwan University, Tainan 710, Taiwan*

Received 2 April 2007; received in revised form 16 October 2007; accepted 23 October 2007
Available online 30 October 2007

**Abstract**

A comb-like polymer was prepared by copolymerization of acrylonitrile and poly(ethylene glycol-methyl methacrylate) (PEGMEM). The copolymer was mixed with a propylene carbonate plasticizer and $LiClO_4$ to form a gel polymer electrolyte (GPE). $^7$Li solid-state NMR analysis was used to elucidate interactions between the lithium ions and unpaired electrons on the gel polymer groups. $^7$Li magic-angle spinning NMR and Fourier-transform infrared spectroscopy revealed that the PEGMEM segment could promote dissociation of the lithium salt. Differential scanning calorimetry was used to study the thermal behavior of GPEs of different compositions. The conductivity increased with PEGMEM content. Furthermore, the conductivity of GPE based on a comb-like copolymer exceeded that based on polyacrylonitrile (PAN) with the same composition (polymer/plasticizer 50:50 wt.%). Notably, the highest conductivity of the copolymer/plasticizer 50:50 wt.% system ($2.51 \times 10^{-3}$ S cm$^{-1}$) was close to that for the PAN/plasticizer 20:80 wt.% system ($1.90 \times 10^{-3}$ S cm$^{-1}$).


*Keywords:* Comb-like; Copolymer; Gel polymer electrolyte

## 1. Introduction

Since Wright and others found that poly(ethylene oxide) (PEO) dissolved salts and had an ionic conductivity of $10^{-8}$ to $10^{-7}$ S cm$^{-1}$ at ambient temperature [1,2], solid polymer electrolytes (SPEs) have attracted considerable attention because of their potential application to various electrochemical devices. A novel polymer material with high ionic conductivity, good mechanical properties and thermal stability for technological application is desirable. However, the conductivity of the polymer electrolyte must reach $1 \times 10^{-3}$ S cm$^{-1}$ for practical applications. Unfortunately, most SPEs do not reach this value. Therefore, polymer–solvent–salt-based electrolytes were developed. These electrolytes, called gel polymer electrolytes (GPEs), have higher conductivity than SPE systems. They retain not only the high conductivity of the liquid electrolyte, but also the good mechanical properties of the polymer matrix.

Among GPEs, the polyacrylonitrile (PAN)-based system has been investigated extensively because of its high conductivity at room temperature and dimensional stability. However, to achieve good conductivity, more plasticizers must be added to the system [3], which reduces the mechanical strength of GPEs. In addition, according to the literatures [4,5], plasticizers are the origin of the continuous growth of a passivating layer through reaction with the Li electrode. Therefore, a GPE matrix is required to solve these problems.

Recently, comb-like polymers with oligomeric PEO in their side chains have attracted interest for use in polymer electrolytes [6–11]. Since the pendant PEO side chains alter the matrix flexibility, fast side-chain motion increases the mobility of the dissolved ions and thus improves their conductivity. The highest conductivity for solvent-free comb-like polymer electrolytes at ambient temperature is approximately $10^{-5}$ S cm$^{-1}$. Therefore, introducing a comb-like PEO into GPEs can decrease the plasticizer content required and maintain the conductivity at $>10^{-3}$ S cm$^{-1}$.

High conductivity and favorable mechanical properties have to be considered in preparing a polymer electrolyte for practical applications. In our previous study, a comb-like PEO was

* Corresponding author. Tel.: +886 6 2757575x62643; fax: +886 6 2360464.
*E-mail address:* ccy7@ccmail.ncku.edu.tw (C.-Y. Chen).

0378-7753/$ – see front matter © 2007 Elsevier B.V. All rights reserved.
doi:10.1016/j.jpowsour.2007.10.069

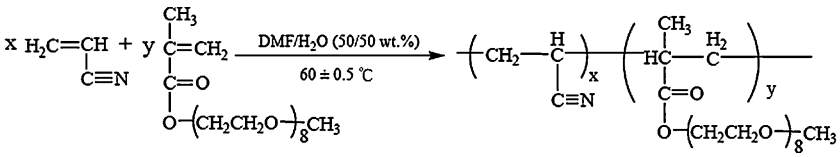


Scheme 1. The reaction equation for poly(AN-co-PEGMEM) copolymer.

introduced into PAN to form a good SPE matrix [11]. However, it did not have higher conductivity, although it did exhibit better mechanical properties. In the present study, the copolymer was further used in a GPE to achieve good conductivity with low-plasticizer content, as well as good mechanical properties. Copolymers of various compositions were synthesized for the GPE matrix. Differential scanning calorimetry (DSC), $^{7}$Li magic-angle spinning (MAS) NMR and ac impedance measurement were used to investigate the effects of the PEO side chains in GPEs.

## 2. Experimental

### 2.1. Materials and experimental procedure

As shown in Scheme 1, the copolymers were synthesized by radical polymerization in a 500-ml four-necked round-bottom flask equipped with an anchor-propeller stirrer under a nitrogen atmosphere. Monomers poly(ethylene glycol-methyl methacrylate) (PEGMEM; Aldrich) and acrylonitrile (AN; Fluka) at molar ratios of 1:0.01, 1:0.05 and 1:0.11, 50 wt.% dimethylformamide (DMF; TEOIA Co. Ltd.) and 50 wt.% distilled water were mixed together. Potassium persulfate (KPS; Fluka) was used as the initiator. The reaction temperature was controlled at $60 \pm 0.5\,^{\circ}$C using a thermostatic water bath. After 24 h of polymerization, the flask was cooled to ambient temperature. The products were extracted in toluene and finally dried under vacuum in an oven. The copolymers are denoted as AP1, AP2 and AP3, as shown in Table 1.

Lithium perchlorate ($LiClO_4$; Fluka) was dried in a vacuum oven prior to use. Propylene carbonate (PC; Fluka) was distilled twice and stored in a dry box. Hybrid films were obtained by dissolving the copolymer, $LiClO_4$ and PC at 90 °C, then casting the solution onto a polytetrafluoroethylene (PTFE) substrate. Films were then heated in a vacuum oven at 80 °C to remove excess PC.

### 2.2. DSC thermograms

Thermal analysis of the GPEs was carried out in a Dupont DSC 2910 differential scanning calorimeter at a heating rate of $10\,^{\circ}\mathrm{C\,min^{-1}}$ from −150 to 150 °C.

Table 1
Composition of copolymers from elemental analysis

| Polymer | Elemental analysis (C/N/H) | Copolymer molar ratio (AN/PEGMEM) |
|---|---|---|
| AP1 | 64.39:20.48:6.41 | $1{:}3.12 \times 10^{-2}$ |
| AP2 | 61.31:13.81:7.33 | $1{:}10.18 \times 10^{-2}$ |
| AP3 | 59.46:9.49:7.82 | $1{:}19.90 \times 10^{-2}$ |

### 2.3. Solid-state NMR measurements

$^{7}$Li MAS NMR spectra with power decoupling were recorded on a Bruker AVANCE-400 NMR spectrometer equipped with a 7-mm double-resonance probe operating at 400.13 MHz for $^{1}$H and 155.5 MHz for $^{7}$Li. Typical NMR experimental conditions were as follows: $\pi/2$ pulse length, 4 μs; recycle delay, 30–150 μs; $^{1}$H decoupling power, 65 kHz; and spinning speed, 3 kHz. Chemical shifts were externally referenced to LiCl solution at 0.0 ppm.

### 2.4. Infrared spectroscopy

Fourier-transform infrared (FT-IR) spectra were recorded at room temperature using a Bio-Rad FT-IR system coupled to a computer. The resolution was $2\,\mathrm{cm^{-1}}$ and 64 scans were recorded for each spectrum in the range 400–4000 $\mathrm{cm^{-1}}$.

### 2.5. Conductivity measurements

The ionic conductivity of the GPEs was determined using an electrochemical cell consisting of the electrolytic film sandwiched between two stainless steel electrodes. The cell was placed inside a thermostat under an Ar atmosphere. Impedance analysis was recorded from 30 to 90 °C using Autolab PGSTAT 30 equipment (Eco Chemie B.V., Netherlands) with frequency response analysis (FRA) software using an oscillation potential of 10 mV from 100 kHz to 10 Hz in a thermostatic cell.

## 3. Results and discussion

### 3.1. Copolymer characteristics

Copolymers of various compositions were synthesized by free radical copolymerization of PEGMEM and AN. Fig. 1 shows FT-IR spectra of the copolymers AP1, AP2 and AP3. All spectra display peaks at 2875, 1730, 1112 and 2242 $\mathrm{cm^{-1}}$ because all the copolymers contain $–CH_3$, carbonyl ester, $–CH_2–O–CH_2–$ and –C≡N groups. Notably, the intensities of the carbonyl ester and $–CH_2–O–CH_2–$ peaks increased with the PEGMEM content, which is consistent with the elemental analysis of the copolymers shown in Table 1. Consequently, the FT-IR spectra and elemental analysis reveal that copolymers with AN and PEG on the side chain were successfully synthesized.

Fig. 2 displays DSC thermograms of the copolymers. AP3 shows a low-temperature endothermic transition at −41 °C and a high-temperature endothermic transition at 62 °C, which correspond to $T_g$ for the PEGMEM and AN segments in the copolymers. The low-temperature $T_g$ value substantially

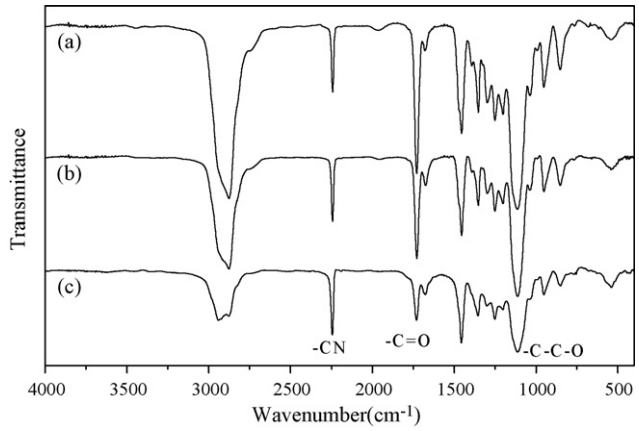


Fig. 1. FT-IR spectra of composite copolymers: (a) AP3, (b) AP2 and (c) AP1.

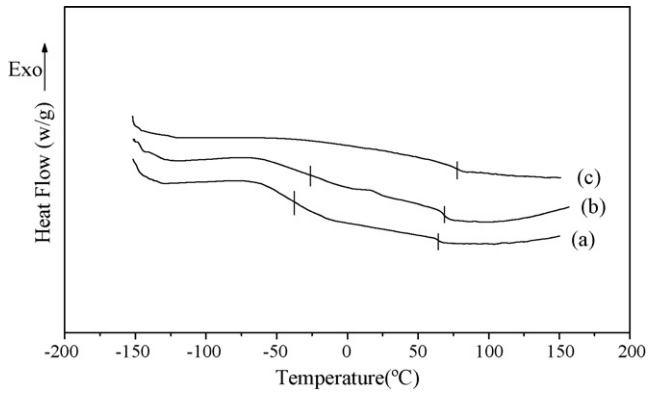


Fig. 2. DSC thermograms of polymers: (a) AP3, (b) AP2 and (c) AP1.

exceeds that of PEGMEM homopolymer (approx. −58 °C) and the high-temperature $T_g$ value is lower than that of PAN homopolymer (approx. 90 °C). These results indicate that the copolymers exhibit a certain degree of mixing of PEGMEM and AN segments.

### 3.2. Lithium ion environment in the gel polymers

Different complexes can be formed by the interaction of different coordination sites of gel polymers with lithium ions, as indicated in Scheme 2. $Li^+$ ions can interact with the oxygen atom of the ether groups, the N atom of C≡N groups, and PC. In the present study, $^7$Li MAS NMR was used to elucidate the interaction of lithium ions with PC, the AN segment and the PEO side chain of PEGMEM. Fig. 3 shows variable-temperature $^7$Li

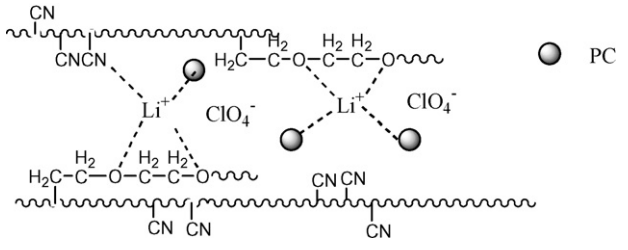


Scheme 2. Schematic representation of complexes formed by the interaction of $Li^+$.

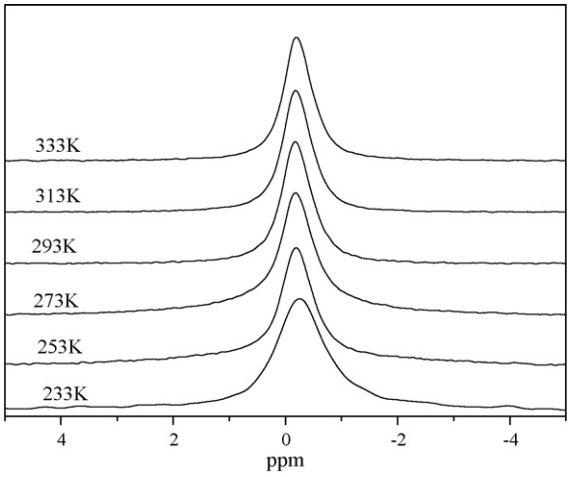


Fig. 3. Variable-temperature $^7$Li proton-decoupled MAS NMR spectra of AP2/PC 50:50 wt.% doped with 0.25 mmol $LiClO_4$ $g^{-1}$ polymer.

proton-decoupled MAS NMR spectra for AP3/PC 50:50 wt.% doped with 0.5 mmol $LiClO_4$ $g^{-1}$ polymer. The spectrum reveals that more than one resonance peak due to various $Li^+$ local environments can be discerned at lower temperatures. An increase in temperature shifted these resonance peaks, which eventually combined to form a single-resonance peak. As discussed in the following section, three resonance sites (1, 2 and 3) are assigned to $Li^+$ ions coordinated to PC, the ether oxygen atom in the PEO side chain, and the nitrogen atom on C≡N groups, respectively. Unlike classical peak merging, which involves a two-site exchange process, the above merging process not only involves a three-site exchange process, but probably also exhibits a temperature-dependent site preference [12–14]. Since three resonance peaks are observed at lower temperatures, the frequency of the exchange process must be greater than the separation of the resonances for effective exchange to occur. At higher temperatures, cation exchange occurs faster than the NMR time scale, resulting in a single-resonance peak with a chemical shift that is the weight average of the individual components.

Fig. 4 shows solid-state $^7$Li NMR spectra for various salt concentrations, obtained at 223 K. Deconvolution of the NMR spectra revealed a mixture of Lorentzian/Gaussian lines for all three resonance peaks. According to literature reports [12,15–17], site 1 is associated with coordination between PC and $Li^+$ ions. Site 2 is attributed to coordination between oxygen atom on the ether groups and $Li^+$ ions, while site 3 is related to coordination between C≡N groups and $Li^+$. At a doping level of 0.25 mmol $LiClO_4$ $g^{-1}$ polymer, site 2 showed the highest intensity resonance peak in the system, indicating that $Li^+$ ions are preferentially coordinated to site 2. The ether oxygen atom in the PEO side chain interacts with the $Li^+$ ions more strongly than the PC and C≡N groups because of the higher donor number of the oxygen atom on PEO. The peak intensities for sites 1 and 3 normalized to the intensity for site 2 increase as a function of the salt concentration, as shown in Fig. 4. Notably, the peak intensity of site 1 is higher than that for site 2 at a doping concentration of 1.0 mmol $LiClO_4$ $g^{-1}$ polymer, indicating that as the salt concentration increases above 1.0 mmol $g^{-1}$ polymer, the amount

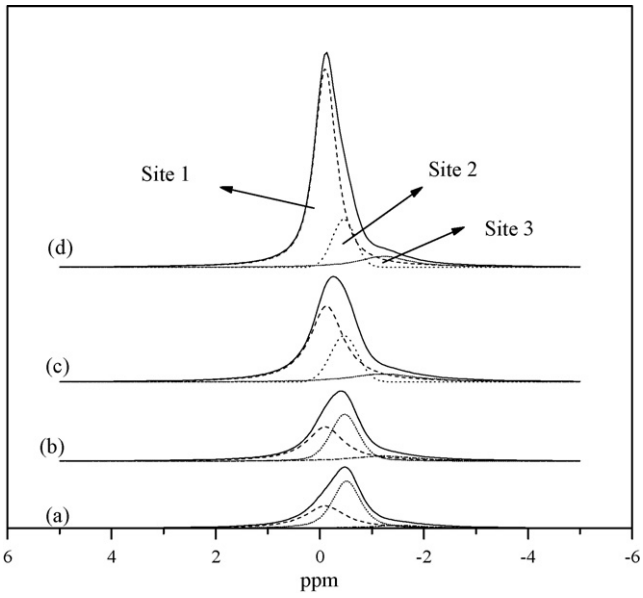


Fig. 4. Deconvolution of $^{7}$Li proton-decoupled MAS NMR spectra at 223 K for AP2/PC 50:50 wt.% doped with (a) 0.25 mmol $LiClO_4$ $g^{-1}$, (b) 0.5 mmol $LiClO_4$ $g^{-1}$, (c) 1.0 mmol $LiClO_4$ $g^{-1}$, and (d) 2.0 mmol $LiClO_4$ $g^{-1}$ polymer.

of $Li^+$ ions dissociated by the PEO side chain approaches saturation. Therefore, the excess $Li^+$ ions then coordinate to PC. This result also affects the GPE thermal characteristics, as confirmed by DSC and discussed below.

Dissociation of the lithium salt is an important parameter that determines the ionic conductivity of the electrolyte. FT-IR is a good tool for probing the degree of dissociation of the lithium salt in different polymer electrolytes. Fig. 5 shows the 580–680 $cm^{-1}$ range of the FT-IR spectrum of the GPE containing 3.0 mmol $LiClO_4$ $g^{-1}$ polymer. The absorption peak can be separated into two components that are centered at 624 and 640 $cm^{-1}$. According to the literatures [18,19], the 624 $cm^{-1}$ band can be attributed to free $ClO_4^-$ and the 640 $cm^{-1}$ band to ion-pair formation or contact of $ClO_4^-$ with $Li^+$. The ratio of the areas of the peaks at 624 and 640 $cm^{-1}$ represents the degree of

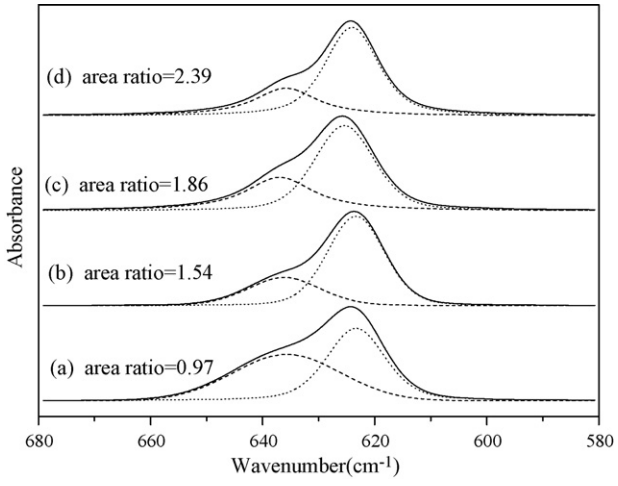


Fig. 5. FT-IR spectra of the perchlorate anion $\nu_4$ band in polymer/PC 50:50 wt.% with $LiClO_4$ (3 mmol $g^{-1}$ polymer): (a) PAN, (b) AP1, (c) AP2 and (d) AP3.

ionization of the lithium salt in the polymer electrolyte. In addition, Fig. 5 reveals that $LiClO_4$ dissociation increased with the PEGMEM content, indicating that PEGMEM can improve the dissociation of lithium salt in electrolytes, and thus the number of charge carriers increases in the system.

### 3.3. Thermal characteristics

It has been reported that dissociation of lithium salts by groups on polymers occurs via the coordination of $Li^+$ ions to unbonded electrons of these groups. Many studies [6,20] have investigated the effect of such coordination on the $T_g$ of polymers. In the present study we employed DSC to elucidate the effect of $LiClO_4$ on GPE thermal transitions. Fig. 6 presents DSC thermograms of the GPEs based on AP3 copolymer with various concentrations of $LiClO_4$. Because of the PC plasticizer, a strong glass-transition step is observed at low temperature. A higher glass-transition temperature is also observed. The transition at lower temperature is assigned to the $T_g$ of PC, and that at higher temperature is assigned to $T_g$ of the AN segment. However, the $T_g$ of PEGMEM is not present in the DSC curve, perhaps for two reasons. First, the PEGMEM $T_g$ may be masked by the range of the glass-transition step for PC. Second, the PEGMEM content is lower than the PC and AN contents, so the transition temperature of PEGMEM is not easily observed. Fig. 7 displays $T_g$ values for the different compositions investigated. $T_g$ for PC and AN increase with the $LiClO_4$ concentration, indicating that $Li^+$ cations are solvated by PC and the C≡N group of the AN segment. The interaction between $Li^+$ ions and polar groups partially impedes local motion of the polymer segment and the PC molecule through the formation of transient crosslinks, increasing $T_g$.

The change in $T_g$ for the GPEs exhibits another interesting phenomenon. Fig. 7(a) shows that at low-$LiClO_4$ concentration, the $T_g$ of PC in the AP1 system varies markedly with $LiClO_4$ concentration; however, $T_g$ remains almost invariant at higher $LiClO_4$ concentrations. The AP3 system does not exhibit this phenomenon. Moreover, the variations with $LiClO_4$ concentration in the AP1 and AP3 systems are opposite, revealing that PEGMEM can increase the dissociation of the lithium salt. In the AP1 system, the lithium ion is mainly coordinated to PC. As

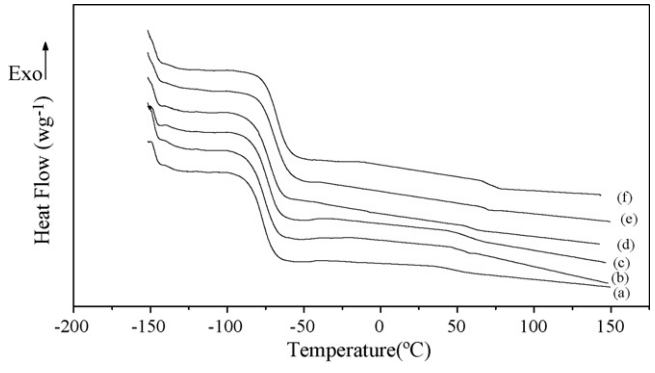


Fig. 6. DSC thermograms for AP3/PC 50:50 wt.% doped with various $LiClO_4$ concentrations: (a) 0.0 mmol $g^{-1}$, (b) 0.25 mmol $g^{-1}$, (c) 0.5 mmol $g^{-1}$, (d) 1.0 mmol $g^{-1}$, (e) 2.0 mmol $g^{-1}$, and (f) 3.0 mmol $g^{-1}$ polymer.

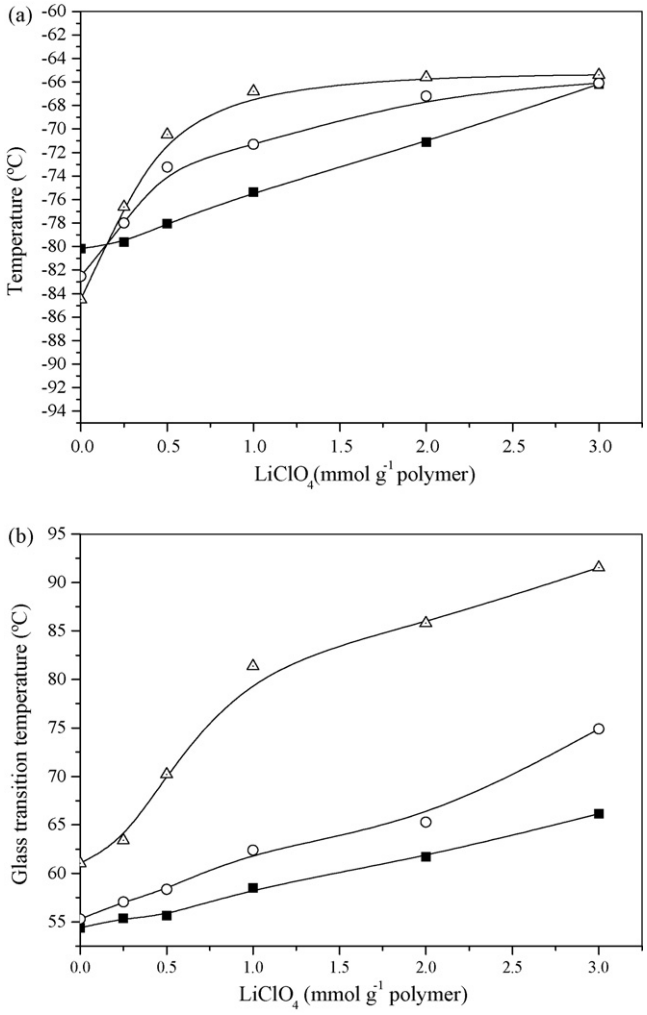


Fig. 7. $T_g$ of (a) PC and (b) AN segment as a function of the $LiClO_4$ concentration for polymer/PC 50:50 wt.%: (■) AP3, (◯) AP2, and (△) AP1.

the $LiClO_4$ concentration increases, the amount of $Li^+$ that is dissociated by PC reaches saturation. Hence, the $T_g$ of PC does not increase with the $LiClO_4$ concentration above a certain level in the AP1 system. In the system with higher PEGMEM content, the PEGMEM interacts with $Li^+$ ions, as confirmed by $^7Li$ MAS NMR and FT-IR. Therefore, the amount of $Li^+$ dissociated by PC does not easily saturate, and the $T_g$ of PC increases slightly with the $LiClO_4$ concentration, even at low levels, in the AP3 system.

### 3.4. Ionic conductivity

The ionic conductivity of GPEs was measured using two stainless steel electrode plates at different temperatures to study the conduction behavior of charge carries in the gel copolymer. Several researchers have reported on the ionic conductivity of comb-like polymer electrolytes [6,20–22] and PAN-based GPEs [3,23–25]. Conductivity varies with temperature according to either the Vogel–Tamman–Fulcher relationship (VTF; Eq. (1)) or the Arrhenius relationship (Eq. (2)), depending on the limits of the temperature range over which the conductivity was

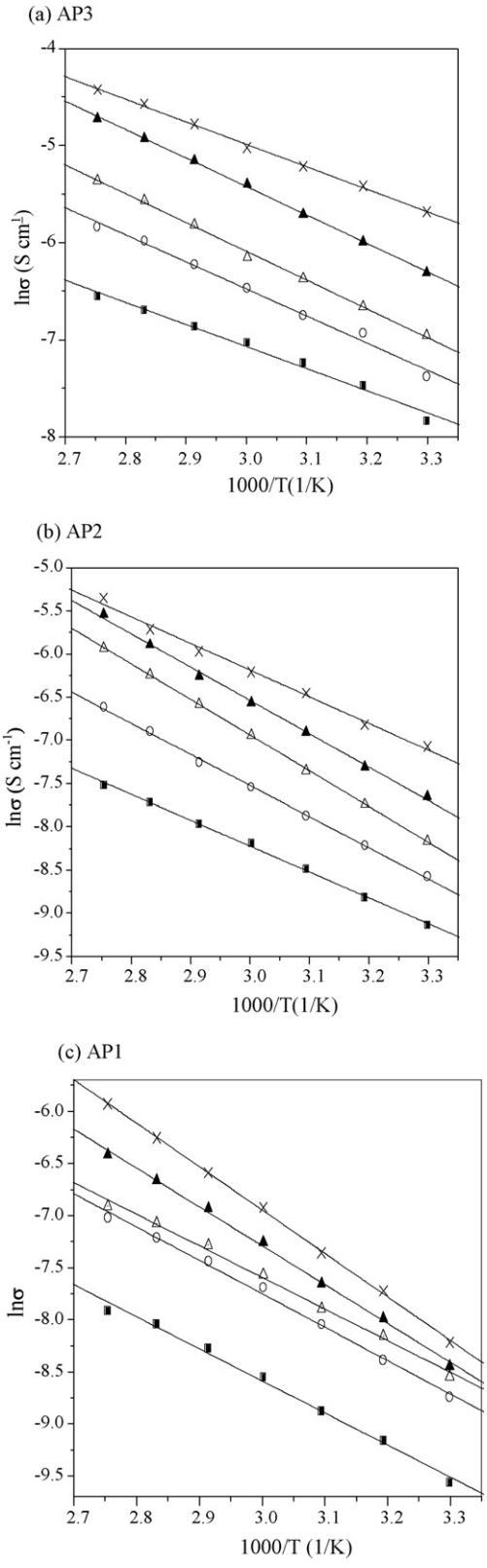


Fig. 8. Arrhenius plots of ionic conductivity for composite gel-type electrolytes polymer/PC 50:50 wt.% doped with various $LiClO_4$ concentrations: (■) 0.25, (◯) 0.5, (□) 1.0, (▲) 2.0 and (×) 3.0 mmol $g^{-1}$ polymer.

Table 2
Activation energy range for conductivity of the gel polymer electrolytes calculated from the Arrhenius equation

| | $E_a$ (kJ mol$^{-1}$) |
|---|---|
| Composition: polymer/PC 50:50 wt.% | |
| AP1 | 26–34 |
| AP2 | 25–32 |
| AP3 | 19–24 |

measured:

$$\sigma = AT^{-1/2} \exp\left[-\frac{B}{k}(T - T_0)\right] \quad (1)$$

$$\sigma = \sigma_0 \exp\left(-\frac{E_a}{kT}\right) \quad (2)$$

where $A$ is a constant that is proportional to the number of carrier ions; $B$ denotes the pseudo-activation energy associated with the motion of the polymer; $k$ is the Boltzmann constant; $E_a$ is the activation energy; $T_0$ is a reference temperature (normally associated with the ideal $T_g$ at which the free volume is zero, or with the temperature at which the configuration entropy becomes zero) [23].

Fig. 8 shows an Arrhenius plot for the electrolyte samples. For all systems, the plot of the ionic conductivity against the reciprocal absolute temperature is linear, confirming that the conductivity follows an Arrhenius relationship with temperature in this temperature range. The Arrhenius relationship indicates that the charge carriers are decoupled from the segmental motion of polymer chain, and the conductive environment of $Li^+$ ions in the GPEs is liquid-like, remaining uncharged in the measurement temperature range. $E_a$ values for the conductivity of the GPEs were calculated from the Arrhenius equation, and are listed in Table 2. Results for $E_a$ conform to the above discussion. The PEO side chain promotes dissociation of the lithium salt in the GPEs. Therefore, $E_a$ decreases as the PEGMEM content increases.

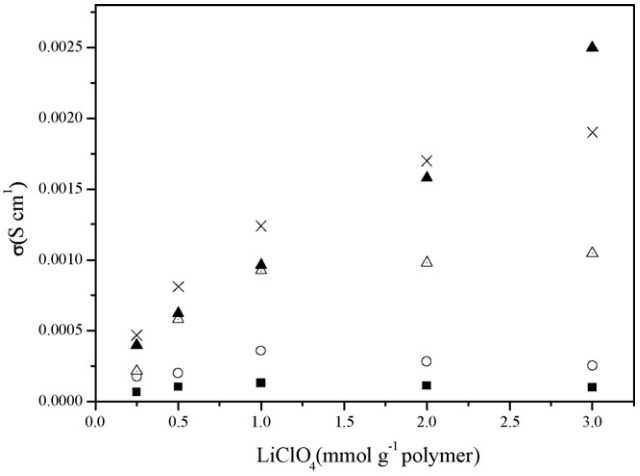


Fig. 9. Ionic conductivity vs. $LiClO_4$ concentration for polymer/PC 50:50 wt.%: (■) PAN, (◯) AP1, (□) AP2, (▲) AP3 and (×) PAN/PC 20:80 wt.%.

Fig. 9 presents the ionic conductivity of all the GPEs studied. The conductivity substantially increases with the number of PEGMEM units in the copolymer. At higher PEGMEM content, the conductivity increases rapidly, even at high $LiClO_4$ concentrations, indicating that the PEGMEM unit can increase the dissociation of the lithium salt and reduce the aggregation of ions in the GPEs, as mentioned above. Thus, the AP3 system exhibits the highest conductivity, $2.51 \times 10^{-3}$ S cm$^{-1}$, which is one order of magnitude greater than that of the PAN system of the same composition. Notably, the ionic conductivity of AP3/PC 50:50 wt.% is close to that of PAN/PC 20:80 wt.%.

## 4. Conclusion

GPEs were synthesized from poly(AN-co-PEGMEM) complexes with PC. $LiClO_4$ was added as the lithium salt to study the conductivity of the GPEs. $^7$Li MAS NMR revealed that the $Li^+$ ions interact with PC and with –C–C–O– and C≡N groups in the gel polymer. DSC indicated that the PEGMEM content and the $LiClO_4$ concentration affect the thermal characteristics of the GPEs. Moreover, the maximum conductivity observed in this study was better than that of a typical PAN-based system of the same composition. Taken together, these results demonstrate that PEGMEM in the copolymer can increase the number of charge carriers, improving the GPE conductivity.

## Acknowledgements

The authors would like to thank the National Science Council of the Republic of China (NSC 95-221-E-006-188) and the Ministry of Economic Affairs of the Republic of China (TDPA: 95-EC-17-A-05-S1-0014), for financially supporting this research. We are also extremely grateful to Ms. Sun for her crucial contribution to solid-state NMR experiments.

## References

[1] P.V. Wright, Br. Polym. J. 7 (1975) 319–327.
[2] B. Armand, Solid-State Ionics 9–10 (1983) 745–754.
[3] M. Watanabe, M. Kanba, K. Nagaoka, I. Shinoara, J. Polym. Sci. Polym. Phys. Ed. 21 (1983) 939–948.
[4] X. Hou, K.S. Siow, J. Solid-State Electrochem. 5 (2001) 293–299.
[5] K.H. Lee, J.K. Park, W.J. Kim, Electrochim. Acta 45 (2000) 1301–1306.
[6] J.S. Gnanaraj, R.N. Karekar, S. Skaria, C.R. Rajan, S. Ponrathnam, Polymer 38 (1997) 3709–3712.
[7] A. Nishimoto, K. Agehara, N. Furuya, T. Watanabe, M. Watanabe, Macromolecules 32 (1999) 1541–1548.
[8] L. Qi, Y. Lin, X. Jing, F. Wang, Solid-State Ionics 139 (2001) 293–301.
[9] S. Pantaloni, S. Paserini, F. Core, B. Serosati, Electrochim. Acta 34 (1989) 635–640.
[10] L. Marchese, M. Andrei, A. Roggero, S. Passerini, P. Prosperi, B. Scrosati, Electrochim. Acta 37 (1992) 1559–1564.
[11] W.H. Hou, C.Y. Chen, Electrochim. Acta 49 (2004) 2105–2112.
[12] H.L. Wang, H.M. Kao, T.C. Wen, Macromolecules 33 (2000) 6910–6912.
[13] W.H. Hou, C.Y. Chen, C.C. Wang, Solid-State Ionics 166 (2004) 397–405.
[14] A. Abragam, The Principle of Nuclear Magnetism, Oxford University Press, Oxford, 1961.
[15] W.H. Hou, C.C. Wang, C.Y. Chen, Polymer 44 (2003) 2983–2991.
[16] B. Huang, Z. Wang, L. Chen, R. Xue, F. Wang, Solid-State Ionics 91 (1996) 279–284.
[17] Y.H. Liang, C.C. Wang, C.Y. Chen, J. Power Sources 148 (2005) 55–65.

[18] N.D. Cvjeticanin, S. Mentus, Phys. Chem. Chem. Phys 1 (1999) 5157–5161.
[19] X. Xuan, J. Wang, J. Tang, G. Qu, J. Lu, Spectrochim. Acta 56 (2000) 2131–2139.
[20] J.S. Gnanaraj, R.N. Karekar, S. Skaria, S. Ponrathnam, Bull. Electrochem. 12 (1996) 738–742.
[21] A. Nishimoto, M. Watanabe, Y. Ikeda, S. Kohjiya, Electrochim. Acta 43 (1998) 1177–1184.
[22] M. Watanabe, T. Endo, A. Nishimoto, K. Miura, M. Yanagida, J. Power Sources 81–82 (1999) 786–789.
[23] K.M. Abraham, M. Alamgir, J. Electrochem. Soc. 137 (1990) 1657–1658.
[24] B. Huang, Z. Wang, G. Li, H. Huang, R. Xue, L. Chen, F. Wang, Solid-State Ionics 85 (1996) 79–84.
[25] F. Croce, S.D. Broen, S.G. Greenbaum, S.M. Slane, M. Salomon, Chem. Mater. 5 (1993) 1268–1272.